Carbon Supported Metal Nanoparticles And Their Electrocatalytic Application For Fuel Cells And Sensor

Aasiya Shaikh and Smrutiranjan Parida*
Department of Metallurgical Engineering and Materials Science, Indian Institute of Technology-Bombay, Powai, Mumbai – 400076, Maharashtra, India
*Corresponding author. Tel: +91-22-2576-7643 E-mail: paridasm@iitb.ac.in (S. Parida)

Abstract:

Noble metal nanoparticles (Pt, Pd, Ag and Au) have attracted much attention due to their excellent electrocatalytic activity for applications such as fuel cells and sensors. These applicationsdemand ultrasmall nanoparticles with large surface area. However, agglomeration at nanoscale limits direct utilization of metal nanoparticles. To overcome this drawback metal nanoparticles are anchored on a suitable support material.

Herein we are demonstrating the enhancement of electrochemical activity of noble metal nanoparticles on two different carbonaceous structures such as particulate carbon nano onions (CNOs) and flat reduced graphene (RGO). Thepalladium-decorated carbon nano-onions (Pd/CNOs) and silver reduced graphene oxide nanocomposite (Ag/RGO) were used as model systems for fuel cell electrocatalyst and electrochemical sensor application, respectively. Highly dispersed, ultrafine Pd nanoparticles (2-4 nm) decorated on CNOs were prepared by a one-step sonochemical method with different Pd loading, without using any reducing agent. The presence of surface functional groups on the CNOs and sonochemical condition help reduction of Pd (II) ions. The electrocatalytic performance of Pd/CNOs were evaluated using formaldehyde oxidation in alkaline media. Similarly, Ag/RGO was synthesized by phytoreduction using leaf extract as green reducing agent to construct a nitrite (NO^{-}) sensor. Ultrasmall silver nanoparticles (2-4 nm) were well dispersed on RGO sheets. Electrochemical investigations indicated that Ag/RGO nanocomposite has excellent catalytic activity towards nitrite oxidation.

Keywords: Fuel cell electrocatalyst, electrochemical sensors, Graphene, Carbon nano-onions and Metal nanoparticles

1. Introduction

Metal nanoparticles with unique physicochemical properties compared to the bulk counterparts. are potential candidate for the electrocatalysis.[1]Various noble metal nanoparticles of Pt, Pd, Ag and Aushow high electrocatalytic activity towards various electrochemical reactions.[2] However high electrochemical activity demands the presence of ultrasmall nanoparticles with large surface area [3]. However with the decrease in size, nanoparticles start to agglomerate due to their high surface energy,which limits direct utilization of metal nanoparticles.[4] To overcome this drawback metal nanoparticles are dispersed on asuitable support material.[5,6]The electrochemical activity of supported metal nanoparticles depends on the proper dispersion of metalnanoparticles

on the support material. Various factors contribute to the dispersion, of which structure of the support and the method of dispersion play an important role. Carbonaceous materialsare ideal support materials for anchoring metal nanoparticles due to their high surface area, chemical inertness, and good electrical conductivity.[7,8]Carbon nanomaterials can be prepared in various morphologies[9]with thetunable surface area,[10]pore size[11] and electronic conductivity.[12,13]In literature extensive research has been carried out to prepare supported metal nanoparticles on various carbon support materials such as activated carbon (AC), carbon nanotubes

(CNT), carbon nanofiber (CNF), mesoporous carbon, carbon nano-onions and graphene.[14–18]Carbon black (Vulcan XC-72) is widely used as a support,however, it has drawbacks such as mass transfer limitations due to its dense structure which prohibits theformation of three phase boundary between gas, electrocatalyst, and electrolyte.[19] In thecase of CNT, metal dispersion on the inert graphitic basal plane surface requires functionalization using strong acids, which significantly reduces electrical conductivity ofsupport.

Carbon nano-onions (CNOs) and graphene provide low ohmic resistance to the charge transport process, and hence accelerate the charge transfer kinetics resulting in high electrocatalytic activity. In graphene and CNOs edge planes of graphitic sheets offers suitable anchoring sites for the metal nanoparticles. These properties make theman effective support material for dispersion of metal nanoparticles.

Here we are reporting thesynthesisand electrochemical performance of highly dispersed Pd nanoparticles decorated CNOs catalysts and silver reduced graphene oxide nanocomposite Ag/RGO. The Pd/CNO were prepared by a simple sonochemical approach, without use of any external reducing agent, and Ag/RGO were prepared by a green synthesis method using leaf extract of Justicia adhatoda (adulsa) as both reducing and stabilizing agent. The CNOs supported nanocatalysts with different Pd loading 18, 28 and 60 wt% were preparedand their electrocatalytic properties were investigated for formaldehyde electrooxidation in alkaline medium. Maximum activity of Pd/CNOs was observed at an optimum composition, which is related to the size effect and distribution of nanoparticles. The Ag/RGO nanocomposite was used for nitrite determination. A maximum sensitivity of $3x10^4$ μA mM^{-1} $cm^{-2}$was obtained for Ag/RGO in 10 nM to 1000 nM concentrationrange.

2. Experimental

2.1. Chemicals andreagents

All chemical reagents were of reagent grade and were used without any further purification. Palladium acetate ($C_4H_6O_4Pd$, 98%), Silver nitrate ($AgNO_3$, 99.9%), potassium chloride (KCl, 99.5 %), sodium chloride (NaCl, 99.9%) and monopotassium phosphate (KH_2PO_4, 99.5%) were purchased from Sigma-Aldrich. Formaldehyde (HCOH, 37%), Sodium hydroxide pellets (NaOH), Nitric acid (HNO_3, 69%) potassium permanganate (KMnO4, 99.9%), hydrogen peroxide (H_2O_2, 30%), hydrochloric acid (HCl, 37%) disodium phosphate (Na_2HPO_4, 99 %), Sodium nitrate ($NaNO_3$,) and sodium nitrite ($NaNO_2$, 99%) and Sulphuric acid (H_2SO_4, 95%) were purchased from Merck Millipore. DI water was used in all experiments at room temperature.

2.2. Synthesis ofnanocomposites

The Pd-decoratedCNO nanoparticleswere synthesized by a simple sonochemical method using a bath sonicator. Briefly, 20 mg of CNO was dispersed in 20 ml of deionized water and sonicated for one hour then an aqueoussolution of the precursor palladium acetate was added gradually to the CNO dispersion with continuous sonication. Pd/CNO nanocomposites with different Pd loading were prepared by changing the concentration of Pd precursor. Similarly for the preparation of Ag/RGO nanocomposite 40 mg of GO was dispersed in 20 ml of ethanol. 6.9 mg of silver nitrate was added to GO suspension, stirred for 30 minutes and then transferred to round bottom flask containing leaf extract. This mixture was then refluxed at 80 °C for 4 hours. Final products were separated by washingseveral times with distilled water followed by ethanol. The nanocomposites were dried overnight in an oven at 60 ^{0}C.

2.3. Characterization ofNanocomposite

The morphology and structure of Pd/CNO nanocompositeswere characterized by high-resolution transmission electron microscope TecnaiG2, F30. X-ray powder diffraction (XRD) patterns were obtained on a Philips X-Pert PRO X-ray diffractogram. All Electrochemical experiments were performed at room temperature using an autolab AUT86445 electrochemical working station. All experiments were conducted using a conventional three-electrode electrochemical cell consisting of glassy carbon electrode (GCE) as working electrode, Hg/Hg_2SO_4 as a reference electrode and a platinum wire as counter electrode. All potentials in the present study are givenversus Hg/Hg_2SO_4 reference electrode at room temperature. Prior to all

electrochemical tests, GCE was activated followed by immobilization of nanocomposites on activated surface.

2. Results anddiscussion

2.1. Characterization of thenanocomposite

Fig.1 shows TEM micrographs of the Pd/CNO nanocomposites with different Pd loading. The micrographsshow auniform distribution of Pd nanoparticles all over the surface of CNO support.

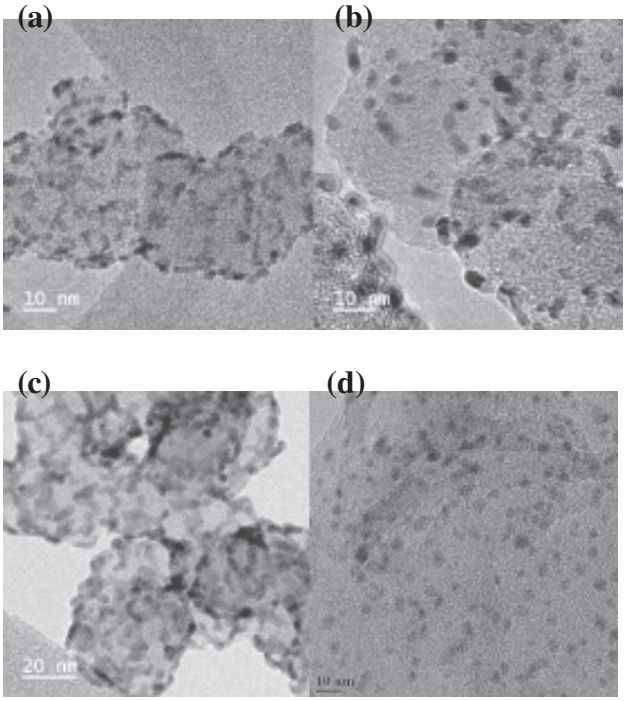


Figure 1: TEM micrographs of the Pd/CNO nanocomposites with increasing Pd loading a) 18 wt%, b) 28 wt%, c) 60 wt% and d) Ag/RGO nanocomposite

The average particle size of Pd varies as 1.8, 2.4 and 4.1 nm for 18 wt%, 28 wt% and 60 wt% of Pd loading in the Pd/CNO composites, respectively. The average particle size does not change significantly up to 28 wt% of Pd loading however at 60 wt% loading the average particle size increased to 4.1 nm with noticeable agglomeration of nanoparticles. The uniform dispersion of Pd nanoparticles on the CNO support can be attributed to the oxygen functionalities present at the surface of CNO nanoparticles, which act as anchoring sites for Pdnanoparticles.

Fig. 1(d) shows the TEM images of the Ag/RGO nanocomposite, spherical silver nanoparticles were well dispersed on reduced graphene oxide sheetswith a size range between 2 and 4 nm. It also suggeststhat leaf extract not only acts as reducing agent but also as an effective capping agent and effectively preventsaggregation of both reduced graphene oxide sheets and silver nanoparticles.

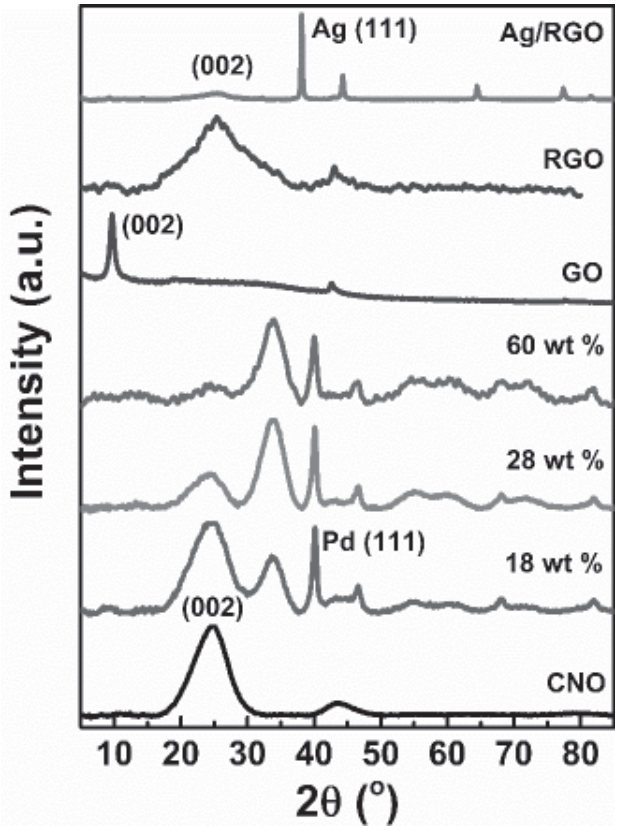


Figure 2: X-ray diffraction of the CNO, Pd/CNO (18 wt %), Pd/CNO (28 wt %), Pd/CNO (60 wt %), GO, RGO and Ag/RGO nanocomposite

The X-ray diffractogram of Pd/CNO and Ag/RGO composites are presented in Fig. 2. The X-ray diffractogram of CNO support (Fig. 2) shows a broad peak at 24.38 corresponding to (002) graphitic plane of CNO. With the increase in the Pd loading in the nanocomposites,the intensity of the characteristic (002) peak of the CNO is diminishing, indicating the formation of increasing number of Pd nanoparticles. At the same time, the characteristic diffraction peaks of Pd are also visible at 40.08, 46.62, 68.02 and 82.03degreescorresponding to (111), (200), (220) and (311) planes of fcc phase of palladium (JCPDS 46-1043).[20]

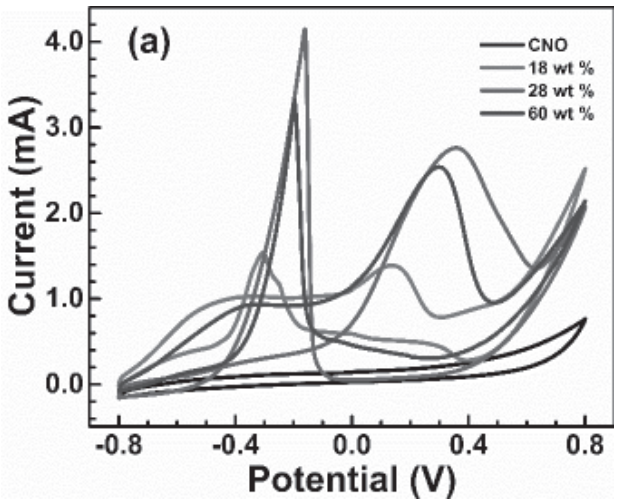
The X-ray diffractogram of GO shows (Fig.2) a strong diffraction peak 20 = 9.68°with a large

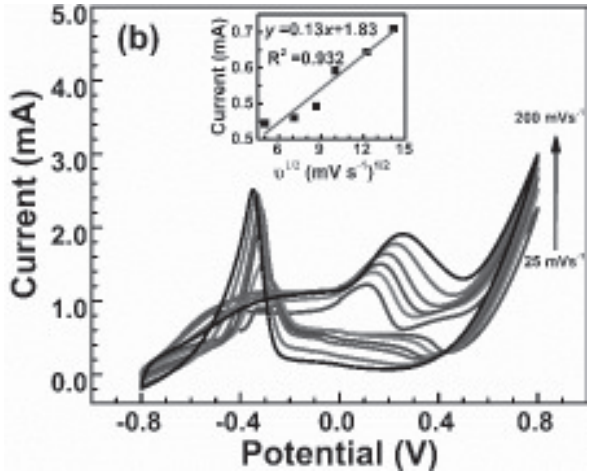
interlayer spacing of 9.12 Å due to the presence of oxygen functional groups on GO (hydroxyl, epoxy and carboxyl groups) as well as water molecules held between the GO sheets. After reduction, XRD of RGO shows a broad (002) peak centered at 25.7 with an interlayer spacing of

3.46 AÚ, suggesting areduction of GO sheets by the leafextract. In Ag/RGO nanocomposite, the appearance of majordiffraction peaks at 38.09°, 44.28°, 64.41°, 77.36° and 81.49°are assigned to the (111),(200), (220) and (311) and (222) planes of silver with the face-centered cubic(FCC) structure.[21] This shows that leafextract simultaneously reduce bothGO and silver salt leading to formation of Ag/RGO nanocomposite.

2.2. Electrochemical activity of Pd / CNOnanocomposites

Electrocatalyticactivities of Pd/CNO nanocomposites were studied using formaldehyde oxidation in the alkaline medium. Fig. 3arepresents cyclic voltammogram (CV) of all nanocomposites and CNO in 0.3 M HCOH in 0.1 M NaOH solution at 50 mVs^{-1}.





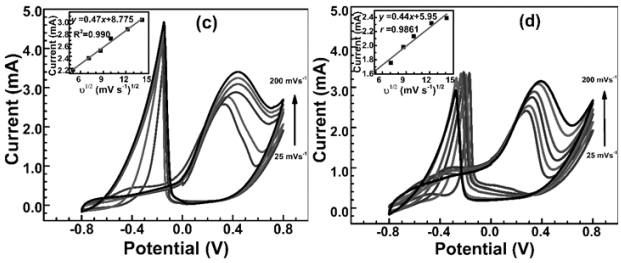


Figure 3: a) cyclic voltammogram (CV) CNO and Pd/ CNO nanocomposites in 0.3 M formaldehyde in 0.1 M NaOH at 50 mVs^{-1} Cyclic voltammograms of Pd/CNO nanocomposites showing the effect of scan rate with increasing Pd loading b) 18 wt%, c) 28 wt% and d) 60 wt% in 0.3M formaldehyde in 0.1M NaOH

The pureCNO does not show any oxidation peaks for formaldehyde, which indicates that pure CNOhas no electrocatalytic activity towards formaldehyde oxidation. In the CV of all the nanocomposites, two distinct anodic peaks are observed in the forward and backward scan, respectively. The absence of reduction peak in cyclic voltammogram indicates the oxidation of formaldehyde at Pd/CNO catalystsis an irreversible process. The peak current density of the forward anodic peak increased with Pd loading up to 28 wt% and then decreased about 20% for 60 wt% Pd loading due to the loading effect, as the particle size increase in this range of loading is insignificant. Consequently, at a 28 wt% of Pd loading an optimum electrochemical activity towards electrooxidation of formaldehyde was achieved. Fig. 3 (b, c and d) shows cyclic voltammogram of all composites in 0.3M HCOH in 0.1M NaOH solution at different scan rates. At all Pd loading, the peak current density of the forward anodic peak increasedas the scan ratewas increased. The inset

graphs in each CVs shows theplot of peak current density of the forward scan against the square root of scan rate. All nanocomposites exhibited a linear relationship between peak current density and thesquare root of scan rate. This linear nature indicates that oxidation is a diffusion controlled process.[22–24]

Fig. 4 (a) shows typical cyclic voltammogram of bare GC, RGO/GCE and Ag-RGO/GC in 0.1 M PBS(pH6.0)inthepresenceof5.0mMNO^- at50mVs^{-1}scanrateinthepotentialrangeof0–

0.7 V. It can be seen that a well-defined oxidation peak is observed at peak potential of 0.45V

for Ag/RGO nanocomposite. This anodicpeak corresponds to the conversion of NO^- toNO^- on

2 3

the surface of Ag/RGO which shows that nanocomposit ehasexcellente lectrocatalytic activity towards the oxidation of NO^-toNO^-. The high anodic current for the electrooxidation of NO^-can be attributed high electro-active surface area of thenanocomposite, strong interfacial interactions and selective adsorption of N atom of NO^- on the Ag nanoparticles.

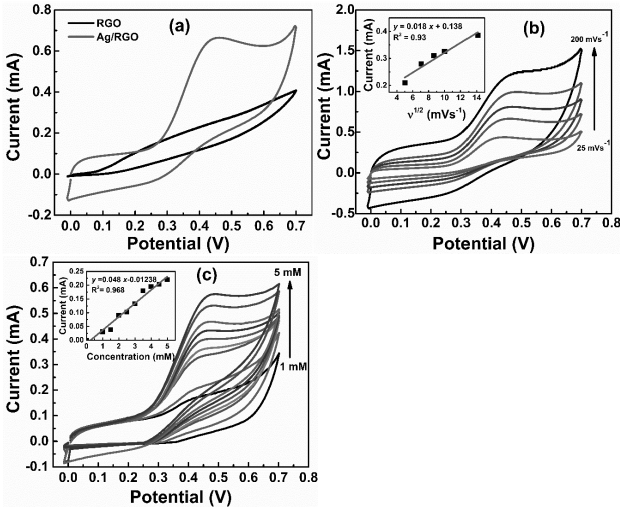


Figure 4: (a) CV response of bare GCE, RGO, and Ag/ RGO nanocomposite in 0.1 M PBS (pH 6.0) in the presence of 5.0 mM NO^- at 50 mVs^{-1}, (b) Series of CVs at different scan rate in 0.1 M PBS (pH 6.0) containing 5 mM NO^- (c) CV response with different concentrations (0.5-5.0mM) of NO^-in 0.1 M PBS (pH 6.0)

Fig.4 (b) represents the effect of different scan rate on the electrocatalytic activity of Ag/RGOin 0.1 M PBS (pH 6.0) containing 5 mM nitrite.The anodic current increases gradually with the increase of the scan rate. The inset of graphs shows anodic peak current increases in a linear relationship with the square root of scan rate and the linear regression line equation can be given as by current (μA) = $27.38v^{1/2}$+44.97 (R^2=0.965). These results reveal that electrocatalytic oxidation of nitrite was diffusion control process.[25] Fig.4 (c) shows the changes to the CV with different concentrations (0.5-5.0mM) of nitrite in 0.1 M PBS (pH 6.0) on the surface of Ag/RGO.The anodic peak current increases with increasing the concentration of nitrite in the solution.The insetof the graph illustrated that the anodic peak current increased linearlywith the concentration of nitrite in the range of 0.5 –5.0 mM. These observations clearly indicated that the Ag/RGO exhibits good catalytic activityand can be used as a sensing electrode for nitrite detection.

4. Conclusion

In the present work,the effect of preparation method, particle size and particle dispersion on the electrochemical activity of various carbon supported noble metal catalysts were discussed. The Pd nanoparticles supported on CNO were synthesized by sonochemical method while Ag/RGO nanocomposite was prepared by phytor eduction using the aqueous leaf extracts of Justicia adhatoda(adulsa) leaf.The electrocatalytic activity of Pd decorated CNO towards formaldehyde oxidation increases with Pd loading up to 28 wt% and further loading decreases the activity, due to nanoparticle agglomeration. The catalyst with 28 wt% of Pd loading shows optimum electrochemical activity with peak current of 125 A/g. The later result demonstrated supported catalysts with ultrafine nanoparticle at high loading can be prepared using CNO as a support. The Ag/RGO exhibited an excellent electrocatalytic activity towards nitrite oxidation and can be utilized as sensor material. Green phytoreduction and facile sonochemical methods are very efficient for the preparation of composite catalyst with excellent electrochemicalperformance.

Acknowledgements

This work was supported by financial assistance from the Industrial Research and Consultancy Center

(IRCC), IIT Bombay. The authors acknowledge access to the experimental facilities at Centre for Research in Nanotechnology & Science (CRNTS), IIT Bombay.

References

1. A. Mohanty, N. Garg, and R. Jin, Angew. Chemie - Int. Ed., 49, 4962–4966(2010).

2. H. You, S. Yang, B. Ding, and H. Yang, Chem. Soc. Rev., 42, 2880–2904 (2013) http://xlink.rsc.org/?DOI=C2CS35319A.

3. M. Sedki, M. B. Mohamed, M. Fawzy, D. a. Abdelrehim, and M. M. S. a.Abdel-Mottaleb, RSC Adv., 5, 17358–17365 (2015) http://xlink.rsc.org/?DOI=C4RA13117G.

4. E. M. Hotze, T. Phenrat, and G. V Lowry, J. Environ. Qual., 39, 1909–1924(2010).

5. M.-Q. Yang, X. Pan, N. Zhang, and Y.-J. Xu, CrystEngComm, 15, 6819–6828 (2013) http://xlink.rsc.org/?DOI=c3ce40694f.

6. C. Tan, X. Huang, and H. Zhang, Mater. Today, 16, 29–36(2013) http://dx.doi.org/10.1016/j.mattod.2013.01.021.

7. H. Huang and X. Wang, J. Mater. Chem. A, 2, 6266–6291 (2014) http://pubs.rsc.org/en/content/articlehtml/2014/ta/c3ta14754a.

8. S. Basri, S. K. Kamarudin, W. R. W. Daud, and Z. Yaakub, Int. J. Hydrogen Energy, 35, 7957–7970 (2010) http://dx.doi.org/10.1016/j.ijhydene.2010.05.111.

9. W. Sun, M. Chen, S. Zhou, and L. Wu, Langmuir, 30, 12011–12017 (2014).

10. H. Liu et al., J. Mater. Chem. A, 1, 12962–12970 (2013) http://www.scopus.com/ inward/record. url?eid=2-s2.0- 84885149464 & partnerI D=40&md5 =36896c1d7051335253d97c025f1c16bc.

11. Z. Xiang-Qian et al., J. Mater. Chem. A, 1, 9449–9455 (2013).

12. A. G. Pandolfo and A. F. Hollenkamp, J. Power Sources, 157, 11–27 (2006). 13. A. Hirsch, Nat. Mater., 9, 868–870 (2010) http://dx.doi.org/10.1038/nmat2885.

14. S. Wu et al., ACS Appl. Mater. Interfaces, 7, 22935–22940(2015).

15. B. Wu, Y. Kuang, X. Zhang, and J. Chen, Nano Today, 6, 75–90(2011).

16. E. S. Steigerwalt, G. A. Deluga, D. E. Cliffel, and C. M. Lukehart, J. Phys. Chem. B, 105, 8097–8101(2001).

17. X.-H. Li and M. Antonietti, Chem. Soc. Rev., 42, 6593–604(2013) http://www.ncbi.nlm.nih.gov/pubmed/23765224.

18. T. Gong et al., J. Phys. Chem. C, 119, 11544–11556 (2015) http://pubs.acs.org/doi/abs/10.1021/jp5130102.

19. M. Yaldagard, World J. Nano Sci. Eng., 3, 121–153 (2013)http://www.scirp.org/journal/Paper Information.aspx? paperID=40507.

20. Y. Zhao, X. Yang, J. Tian, F. Wang, and L. Zhan, Int. J. Hydrogen Energy, 35, 3249–3257 (2010)http://dx.doi.org/10.1016/j.ijhydene.2010.01.112.

21. K.-C. Hsu and D.-H. Chen, Nanoscale Res. Lett., 9, 193 (2014)http://www.pubmedcentral.nih.gov/ articlerender.fcgi?artid=4005903 &tool= pmcentrez & rendertype=abstract.

22. V. Selvaraj, M. Alagar, and K. S. Kumar, Appl. Catal. B Environ., 75, 129–138(2007).

23. B. Habibi and N. Delnavaz, Int. J. Hydrogen Energy, 35, 8831–8840 (2010) http://dx.doi.org/10.1016/j.ijhydene.2010.05.129.

24. Y. Chen et al., Anal. Methods, 5, 3915 (2013)http://xlink.rsc.org/?DOI=c3ay40364e.

25. Z. Wang, F. Liao, T. Guo, S. Yang, and C. Zeng, J. Electroanal. Chem., 664, 135–138 (2012)http://dx.doi.org/10.1016/j.jelechem.2011.11.006.